tvst

Article

Macular Pigment in Eyes With Macular Hole Formation and Its Change After Surgery

Akira Obana[1,2], Risa Nakazawa[1], Saki Noma[1], Hiroyuki Sasano[1], and Yuko Gohto[1]

[1] Department of Ophthalmology, Seirei Hamamatsu General Hospital, Hamamatsu City, Shizuoka, Japan
[2] Department of Medical Spectroscopy, Institute for Medical Photonics Research, Preeminent Medical Photonics Education & Research Center, Hamamatsu University School of Medicine, Hamamatsu, Shizuoka, Japan

Correspondence: Akira Obana, Department of Ophthalmology, Seirei Hamamatsu General Hospital, 2-12-12 Sumiyoshi, Naka-ku, Hamamatsu City, Shizuoka, 430-8558, Japan. e-mail: obana@sis.seirei.or.jp

Received: July 1, 2020
Accepted: October 2, 2020
Published: October 26, 2020

Keywords: macular pigment; macular hole; Müller cell cone; outer plexiform layer

Citation: Obana A, Nakazawa R, Noma S, Sasano H, Gohto Y. Macular pigment in eyes with macular hole formation and its change after surgery. Trans Vis Sci Tech. 2020;9(11):28, https://doi.org/10.1167/tvst.9.11.28

Purpose: To observe the macular pigment (MP) appearances in eyes with macular hole (MH) and clarify the origin of the appearances. The mechanisms underlying the development of MH are discussed based on the observation of MP.

Methods: This observational case series included 33 eyes of 31 patients with MH who underwent vitrectomy. The MP optical density was measured using the two-wavelength fundus autofluorescence technique. The exact localization of MP was evaluated by comparing MP distribution images and optical coherent tomography B-scan images.

Results: MP was missing at the MH. The area of the MP defect corresponded with the area of the defect of outer plexiform layer. MP was present in the retinal flap in stage 2 MH that included glia (Müller cells) and plexiform layers and in the operculum in stage 3 MH, which mainly comprised Müller cells. Cystic spaces in the outer plexiform layer surrounding stage 3 and 4 MHs showed a honeycomb appearance on MP images. MP reappeared to form an irregularly shaped pigment plane after surgical closure of MH. The MP optical volume did not change before and after surgery. Fellow eyes with a central dip in MP distribution subsequently developed MH.

Conclusions: The characteristic appearances of MP at the MH were attributed to MP in the plexiform layers and Müller cell cones. A central dip of MP distribution might be a sign of Müller cell cone damage that proceeds with MH formation.

Translational Relevance: Observation of MP was useful for understanding the mechanisms of MH formation.

Introduction

A histologic study of monkey eyes[1] showed that macular pigment (MP), consisting of xanthophyll carotenoids, is largely present in the Henle fibers layer, which is the foveal portion of the outer plexiform layer (OPL) that is composed of the axons of the cone photoreceptors. Some MP is also present in the inner plexiform layer (IPL) and nerve fiber layer. A histologic study of human eyes[2] showed that the inner half of the foveola is composed of an inverted cone-shaped zone of Müller cells, named the Müller cell cone by Gass.[3] Gass hypothesized that the Müller cell cone was a reservoir for MP, and it played a primary role in macular hole (MH) formation. There has been no direct evidence of xanthophyll carotenoids in Müller cells, but our previous study on MP in lamellar MH cases showed indirectly that Müller cells contained carotenoids.[4] We hypothesized that MP is composed of two parts: MP in the Müller cell cone in the foveal center (foveola) and MP in the plexiform layers (largely in the Henle fibers layer) at the fovea.

Neelam et al.,[5] using resonance Raman spectroscopy, first showed that MH lacked MP and that the MP reaccumulated after successful surgical closure of the MH. A recent study using the autofluorescence technique suggested that reaccumulation of MP might be due to the reapposition of the edge of the MH.[6] These studies investigated the relationship between the amount of MP and visual prognosis, but no definite correlations were obtained.

The amount of MP and its distribution differs largely among individuals.[7–10] We classified MP

distribution patterns into four types[11]: central peak distribution, ring-like distribution, plateau distribution, and central-dip distribution. We speculated that a central-dip distribution, comprising low MP volume at the foveal center, represented some damage to Müller cells, as also reported by others.[12]

In the present study, we investigated MP appearances in MH cases and observed the postoperative changes in MP for up to 2 years, with a view to discerning the origin of the MP appearances. We discuss the possibility that a central-dip distribution of MP is a predictor of MH development.

Methods

Surgical Procedure

This observational study included 33 eyes of 31 patients (17 men and 14 women) with idiopathic MH who underwent vitrectomy. Patients were aged 40 to 81 years (mean ± SD = 69.1 ± 7.7 years). All eyes had no ophthalmoscopically apparent pathology, other than MH, on the macular area. All subjects underwent 25-gauge vitrectomy. The internal limiting membrane (ILM) was peeled off all around the MH by microforceps using the triamcinolone-assisted technique in 26 eyes. No staining agents were used. The inverted ILM flap technique[13] was used in five eyes, and autologous transplantation of the ILM[14] was performed in two eyes. Air tamponade was used. Successful closure of the MH was achieved in all eyes with the first operation in this study. The phakic eyes (26 eyes) underwent phacoemulsification with intraocular lens implantation combined with MH surgery.

This study was approved by the institutional review board of Seirei Hamamatsu General Hospital (No. 2198). All subjects provided written informed consent that complied with the tenets of the Declaration of Helsinki.

Ophthalmologic Examinations and Observations of MP Distribution

Patients underwent visual acuity measurement using a decimal visual acuity test chart and spectral domain optical coherence tomography (OCT, Spectralis OCT, Heidelberg Engineering Inc., Heidelberg, Germany) testing before and after surgery. On preoperative OCT images, the minimum and maximum sizes of the MH and the size of defect of the OPL at the MH were measured in horizontal and vertical line scans using SPECTRALIS software (Fig. 1A). Because the determination of the edge of the OPL at the MH was difficult and prone to subjective bias, three investigators (AO, RN, SN) measured it blinded to MP images; the average of the three values was used for further analysis. In postoperative OCT images, we evaluated three findings: elevation or cystoid space in the outer retinal layers, recovery of the external limiting membrane (ELM), and recovery of the ellipsoid zone.[15–18] The follow-up period was 2 years in 10 eyes, 1 year in 16 eyes, 6 months in 6 eyes, and 2 months in 1 eye.

The MP optical density (MPOD) was measured by the two-wavelength (486 nm and 518 nm) fundus autofluorescence technique, before and after surgery. The prototype MPOD module on the Heidelberg SPECTRALIS with MultiColor (SPECTRALIS-MP, Heidelberg Engineering Inc.) was used. The basic mechanism and handling of this instrument are described elsewhere.[19,20] The pupil was dilated to at least a diameter of 7 mm using a topical mydriatic agent. The reference point was set to 9° eccentricity. The sum of all MPOD values in the area of a 9° radius (MP optical volume [MPOV]) was measured.[21] The MPOD is dimensionless, so the MPOV is unitless as well. The transverse size of the OCT B-scan and MP images was adjusted, SPECTRALIS OCT B-scan images were imposed on the MP images, and the exact layers in which the MP existed in the retina were evaluated. Using preoperative MP images, the maximum diameter of the central MP defect in the horizontal and vertical axes were measured using Image J (v 1.52, National Institutes of Health, Bethesda, MD).

Statistical Analyses

Statistical analyses were performed using Statistical Package for Service Solution (SPSS) software, version 25 (IBM SPSS, Chicago, IL), and the significance level was set at a P value of less than 0.05. Comparisons of two average values of numerical variables were performed using t-tests, and correlations between two numerical variables were investigated using Pearson's correlation coefficient tests. The MPOV at different time points was analyzed using one-way analysis of variance.

Results

Anatomic and Functional Outcomes

Before surgery, 1 eye had stage 1, 6 eyes had stage 2, 10 eyes had stage 3, and 16 eyes had stage 4 MHs according to Gass' classification.[22] Decimal best-corrected visual acuity (BCVA) ranged from

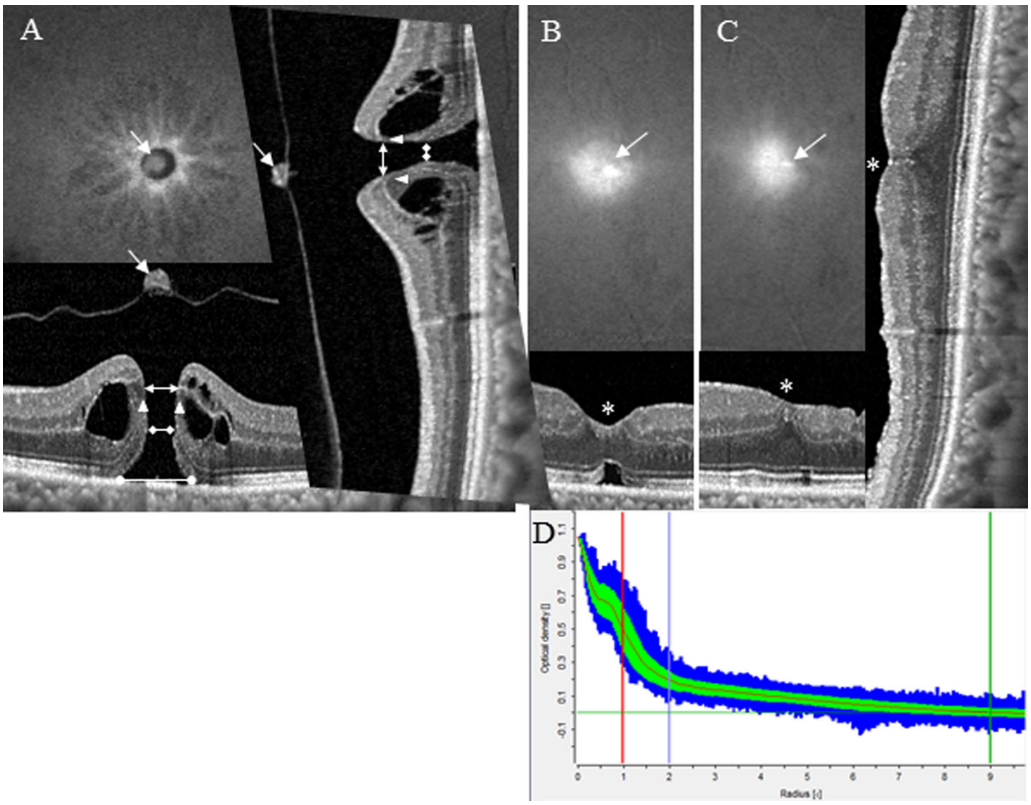

Figure 1. Stage 3, MH, left eye. MP distribution image and OCT images of horizontal and vertical line scan. (A) Before surgery. A defect of the MP corresponds with the diameter of the defect of OPL (*double-headed arrow*). Two *arrow heads* indicate the edge of the OPL defect. The operculum (*arrows*) contains MP. The honeycomb appearance of the MP surrounding the MH corresponds with cystic spaces in the OPL. The *double-diamond line* and *double-circle line* indicate the minimum and maximum size of the MH, respectively. Visual acuity was 0.3. (B) Two weeks after surgery. Dense pigment spot (*arrow*) is considered to correspond with glia at the foveal center (*). Cystic space is observed in OCT images. Visual acuity was 0.6. (C) One year after surgery. The dense pigment spot (*arrow*) is considered to correspond with glia at the foveal center (*), but the size of dense pigment spot is smaller than that at 2 weeks after surgery. A tiny cystic space is noted in OCT images. Visual acuity was 1.2. D. The mean MPOD profile at 2 weeks after surgery. The distribution showed a central peak pattern.

Table 1. OCT Findings After Surgery

	2 Weeks	1 Month	3 Months	6 Months	12 Months	24 Months
No. of eyes	33	33	33	32	26	10
Absence of the cystoid space (%)	20 (61)	22 (67)	26 (79)	24 (75)	20 (77)	9 (90)
Reestablishment of the ELM integrity (%)	20 (61)	23 (70)	26 (79)	27 (84)	23 (88)	10 (100)
Reestablishment of the ellipsoid zone integrity (%)	2 (6)	2 (6)	9 (27)	16 (50)	15 (57)	8 (80)

0.08 to 1.2 (log minimum angle of resolution, –0.08 to 1.10; mean ± SD, 0.48 ± 0.30). The BCVA at the final visit ranged from 0.3 to 1.2 (log minimum angle of resolution, –0.08 to 0.52; mean ± SD: 0.05 ± 0.16). Figure 2 shows the gradual postoperative improvement in BCVA with time.

On OCT images, MH closure was achieved in all eyes. The rate of cystoid space existence in the outer retinal layers, reestablishment of the ELM, and reestablishment of the ellipsoid zone with time are shown in Table 1. All three abnormalities recovered with time. There were no significant differences in MPOV between eyes with and without these abnormalities at every time point from week 2 to year 2 (*t*-test; we excluded analysis of the ELM at year 2 because the ELM was reestablished in all eyes [data not shown]). There were no significant correlations between BCVA and MPOV at any time point from week 2 to year 2 (Pearson's correlation test [data not shown]).

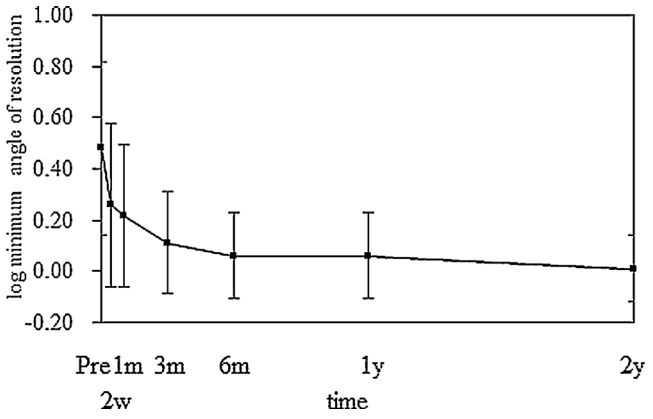

Figure 2. Change in the mean BCVA. Visual acuity improved with time after surgery.

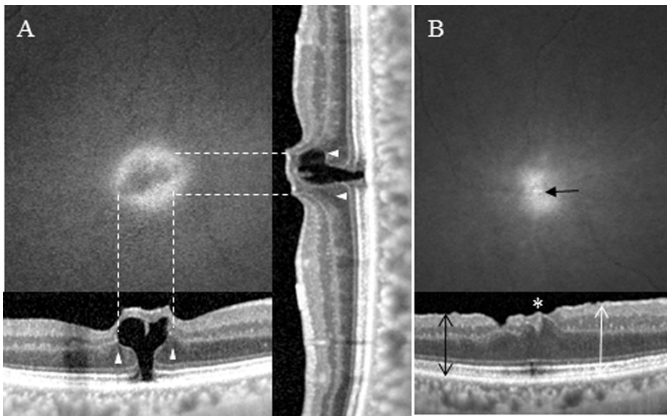

Figure 3. Stage 1 MH, right eye. MP distribution image and OCT images of horizontal and vertical line scans. (A) Before surgery. A defect of MP corresponds with the diameter of the defect in the OPL (between the two *dashed lines*). *Arrow heads* indicate the edge of the OPL defect. Visual acuity was 0.6. (B) One year after surgery. The MH was closed with an irregularly shaped foveal curvature. The defect of MP disappeared. A dense pigment spot (*arrow*) is considered to correspond with the glia at the center of the fovea (*). The thickness of the retina is thinner on the temporal side (*black double-headed arrow*) than on the nasal side (*white double-headed arrows*). The visual acuity was 1.2.

Characteristics of MP Before Surgery

The characteristic finding was the defect of MP at the MH. This defect was noted in all eyes, irrespective of the stage of MH (Figs. 1A, 3A, 4A, and 5A). The diameter of the area of the MP defect was 115 to 675 µm in the horizontal line and 166 to 575 µm in the vertical line. The mean diameter of the area of the MP defect of the MH, the mean minimum and maximum diameters of the MH, and the mean diameter of the defect of the OPL are shown in Table 2. We calculated the concordance rates between the minimum and maximum diameters of the MH, the mean diameter of the OPL defect, and the mean diameter of the MP defect. The correspondence rate between the diameters of the OPL defect and the MP defect (shown in bold in Table 2) was closer to 1 than was the correspondence rate with the minimum and maximum diameters in stages 1, 3, and 4 MH. In stage 2, the correspondence rate between the diameters of the OPL defect and the MP defect was lower than at other stages. The diameter of the area of the MP defect of the MH, the minimum diameter of the MH, and the maximum diameter of the MH were significantly associated with preoperative BCVA and final BCVA (Table 3).

In all six eyes with stage 2 MH, the retinal flap demonstrated MP (Fig. 4A). In OCT images, the retinal flap included tissue, which was presumed to be glia (a part of the Müller cell cone), at the tip and OPL underneath the flap. Identification of the IPL was difficult because of the limited resolution of the OCT image. Operculum was present in nine of 10 eyes with stage 3 MH. All opercula contained MP (Fig. 1A). Lamellar hole-associated epiretinal proliferation[23] was identified in five eyes, and MP was noted in the lamellar hole-associated epiretinal proliferation in four of these five eyes (Fig. 5A). Lamellar hole-associated epiretinal proliferation in one eye was so small that no MP was observed. In the area surrounding the MH, 31 eyes showed a honeycomb MP appearance, which corresponded with the cystic spaces in the OPL in OCT images (Figs. 1A and 5A).

Characteristics of MP After Surgery

MP reappeared in all eyes at the first measurement of MP after surgery (Figs. 1B, 4B, and 5B). However, MP was distributed in an irregularly shaped plane with a dense pigment spot (Figs. 1B, 1C, 3B, 4B–4D, and 5C–5E) and a hypopigmented patch in the plane (Figs. 4B–D and 5C, 5D). A dense pigment spot was usually observed at or near the foveal center, although the exact location of the foveal center was difficult to determine. The hypopigmented patch corresponded to the area of the OPL defect (Figs. 4B–4D). In 21 cases, a hypopigmented patch appeared in the MP plane later than month 3 and disappeared by years 1 or 2 (Fig. 5).

Figure 6 shows a change in the mean MPOV of all eyes after surgery. We compared the mean values statistically in seven eyes that received MPOV at month 1, month 3, year 1, and year 2. There were no significant differences in the mean MPOV at the different time points ($n = 7$; $P = 0.724$, one-way repeated analysis of variance). Because the MPOD before surgery was underestimated because of cataract, it was inappropriate to compare the values before and after surgery directly with the presurgical values in the eyes with cataract. Therefore, the change in the mean MPOV

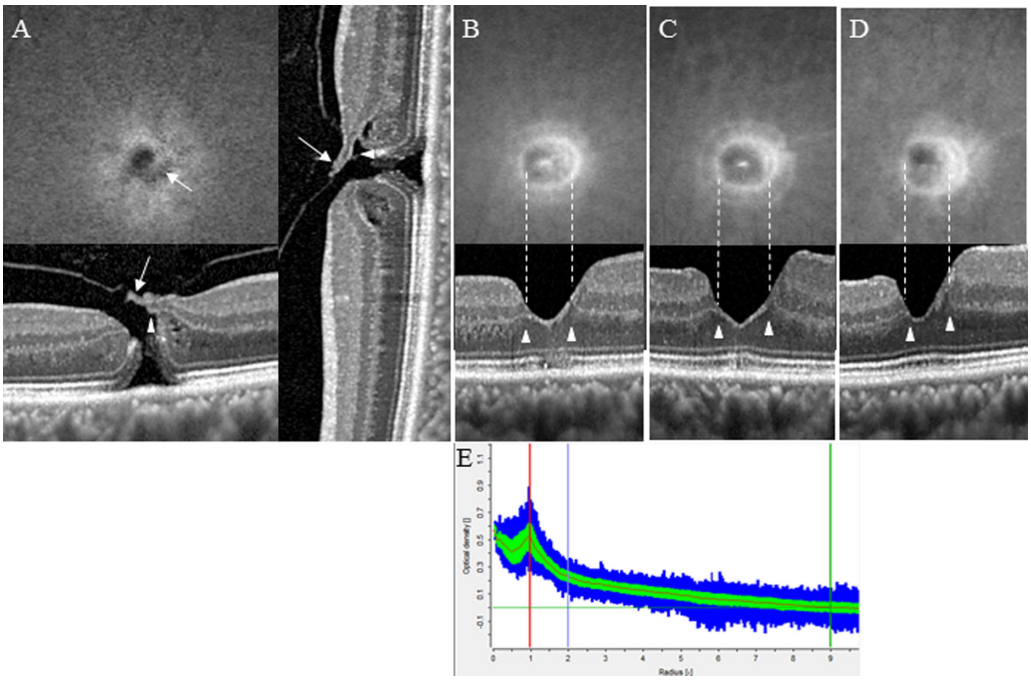

Figure 4. Stage 2 MH, right eye. MP distribution image and OCT images of horizontal and vertical line scans. (A) Before surgery. A defect of MP is observed. The retinal flap (*arrows*) contains MP. Note that the retinal flap contains glia at the tip of the flap and OPL on the bottom of the flap (*arrow head*). The visual acuity was 0.5. (B) Two weeks after surgery. The visual acuity was 1.0. (C) Three months after surgery. The visual acuity was 1.0. (D) Two years after surgery. The visual acuity was 1.2. (B–D) A central dense pigment spot and surrounding ring-like pigment is noted. The MP distribution and shape of the foveal defect shown in OCT images changed from week 2 through year 2; however, the diameter of the low pigment area always corresponded with the defect of the OPL (between the two *dashed lines*). *Arrow heads* indicate the edge of the OPL. (E) The mean MPOD profile with SDs (green bars) and maximum and minimum values (*blue bars*) at 2 weeks after surgery. The distribution showed a ring-like pattern. The peak of the ring located at 1° eccentricity.

Table 2. Mean Diameter of the Central Defect of MP and Its Concordance With the Minimum and Maximum Diameters of the MH, and the Diameter of the Defect of the OPL in Every Stage of MH

		Horizontal Section (μm)				Vertical Section (MM)			
	No. of Eyes	Mean Minimum MH Diameter	Mean Maximum MH Diameter	Mean Diameter of the OPL Defect	Mean Diameter of the MP Defect	Mean Minimum MH Diameter	Mean Maximum MH Diameter	Mean Diameter of the OPL Defect	Mean Diameter of the MP Defect
Stage 1	1	186	258	655	671	115	229	404	407
Rate of concordance		3.6	2.60	**1.02**	–	3.54	1.78	**1.01**	–
Stage 2	6	300	758	250	295	282	661	229	282
Rate of concordance		1.26	0.51	1.43	–	1.63	0.63	1.39	–
Stage 3	10	249	714	387	351	258	613	364	337
Rate of concordance		1.61	0.53	**0.90**	–	1.35	0.59	**0.93**	–
Stage 4	16	378	889	455	423	342	783	419	398
Rate of concordance		1.3	0.55	**0.96**	–	1.34	0.57	**0.98**	–

The rate of concordance was calculated as the diameter of the central MP defect divided by the minimum or maximum MH diameter, or the diameter of the OPL defect. The values in bold demonstrate the correspondence rate between the diameters of the OPL defect and the MP defect.

before and after surgery was analyzed in eyes that had been pseudophakic before MH surgery (Fig. 7). We compared the mean values statistically in five eyes that received MPOV before surgery, at month 3, month 6, and at year 1. There were no significant differences in the mean MPOV at the different time points (n = 5; $P = 0.352$, one-way repeated analysis of variance).

The MP volume was compared between the nasal and the temporal sides in 24 eyes at year 1. The sum of MPOD values in the flabellate area of 135° on the nasal side, from the center, ranged from 4274 to 10,957 (mean ± SD, 6793 ± 1960), and that in the flabellate area of 135° on the temporal side ranged from 2639 to 11,037 (mean ± SD = 5702 ± 2268). The mean volume

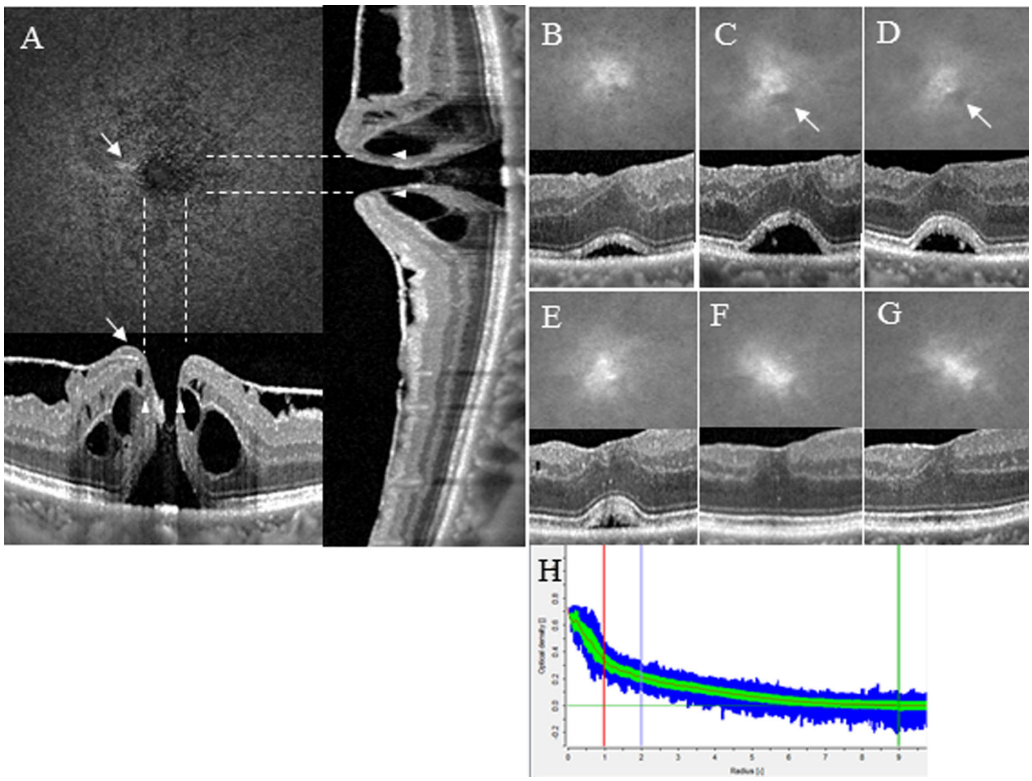

Figure 5. Stage 4 MH, right eye. MP distribution image and OCT images of horizontal and vertical line scans. (A) Before surgery, a defect of MP corresponds with the diameter of the defect of the OPL (between the two *dashed lines*). *Arrow heads* indicate the edge of the OPL defect. Lamellar hole-associated epiretinal proliferation (*arrows*) contains MP. The honeycomb appearance of the MP surrounding the MH corresponds with cystic space in the OPL. The low contrast of the MP was because of cataract. The visual acuity was 0.3. (B) Two weeks after surgery. (C) One month after surgery. (D) Three months after surgery. (E) Six months after surgery. (F) One year after surgery. (G) Two years after surgery. The visual acuity was 1.2. (B–G) The shape of the pigment plane changes with time. A low pigment patch (*arrow*) appears from month 1 to month 3 and extinguished at month 6 and later. Cystoid space is noted from week 2 to month 6. (H) The mean MPOD profile at 2 weeks after surgery. The distribution showed a central peak pattern.

Table 3. Pearson Correlation of the Diameter of the MP Defect, Minimum Diameter of the MH, and Maximum Diameter of the MH, with the BCVA Before and After Surgery (Pearson's Correlation Coefficient Is Shown)

	Diameter of MP Defect	Minimum Diameter of MH	Maximum Diameter of MH
BCVA before operation	0.384, $P = 0.027$	0.559, $P = 0.001$	0.546, $P = 0.001$
BCVA at the final visit	0.500, $P = 0.003$	0.571, $P = 0.001$	0.360, $P = 0.039$

The diameter used in this statistic was the mean value of the horizontal and vertical values.

of MPOD on the nasal side was significantly higher than that on the temporal side ($P < 0.0001$, paired *t*-test).

MP in Fellow Eyes

We investigated MP in the fellow eyes of 25 subjects. The MPOD could not be measured in the fellow eyes of eight subjects because of the following reasons: three had a dense cataract, four had a MH, and one had a history of vitrectomy. We classified the distribution type into four categories based on our previous report[11] and found that two showed the central peak type, five showed the ring-like type, eight showed the intermediate type, and 10 showed the central-dip type (Figs. 8 and 9). In the 10 eyes with the central-dip type, ERM was present in one eye, lamellar MH was present in one eye, and an abnormal asymmetric contour of the foveal defect and/or irregular hyperreflective dots was noted in eight eyes (Fig. 8C). OCT revealed complete PVD in 5 of these 10 eyes, and 3 of them had pseudo-opercula on the detached posterior vitreous membrane.

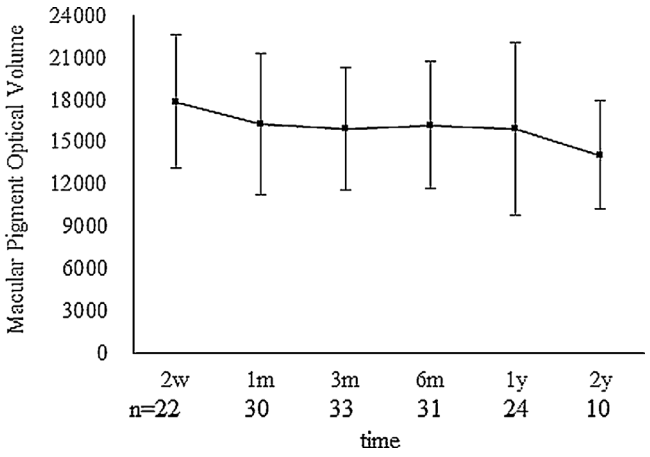

Figure 6. A change in the mean MPOD volume of all eyes. No remarkable change is noted.

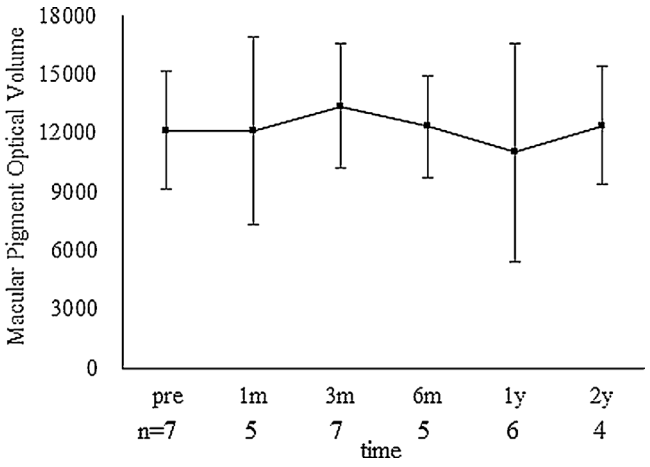

Figure 7. A change in the mean MPOD volume from before to after the operation in all eyes that had been pseudophakic before MH surgery. No remarkable change is noted between before and after surgery.

Follow-up examination in the fellow eyes showed that a central dip developed with the progression of PVD (Fig. 8), and an eye with a central-dip MP distribution developed a MH (Fig. 9).

Discussion

MP was missing at MHs of all stages and recovered after successful surgery. The area of the MP defect at the MH corresponded to the area of the OPL defect. The retinal flap, including plexiform layers in stage 2 MH, contained MP (Fig. 4A). The honeycomb appearance of MP surrounding the MH corresponded to cystic spaces in the OPL[15] (Figs. 1A and 5A). These appearances are thought to be caused by MP in the plexiform layers, particularly in the OPL. The retinal flap in stage 2 MH and operculum in stages 3 MHs contained Müller cells,[24] and they contained MP. This result suggests that the Müller cell cone contains MP. Consequently, the present results support our hypothesis that MP is largely localized in the OPL and Müller cell cone. The shape of MP plane after surgery changed with the tissue repair by Müller cell proliferation and reconstruction of sensory systems, but the MPOV did not differ before and after surgery. MPOV did not correlate with BCVA or pathologic changes in the outer retina. A fellow eye developed PVD with pseudo-opercula containing MP, and the MP distribution type of this eye changed from the ring-like type to the central-dip type. This result implies that a part of the Müller cell cone was damaged with PVD, and a central dip was formed. Another eye with a central dip and incomplete PVD developed MH. Therefore, the central-dip type MP distribution might be a sign of Müller cell damage that could advance to MH development.

A previous histologic study in monkey eyes[1] showed that MP is present in the plexiform layers, and a recent study in human eyes showed that the MP was largely localized in the foveal OPL as well as in the IPL and outer nuclear layer.[25] The characteristics of the MP appearance in MHs are well explained by the concept that MP is mainly localized in the OPL. However, the present findings do not deny the localization of MP in other layers, such as the IPL. We did not evaluate the diameter of the IPL defect. The diameter of the IPL defect seemed to resemble that of the OPL defect in many cases. The corresponding rates between the diameter of the MP defect and the OPL defect were high in stages 1, 3, and 4 MHs, but these rates were relatively low for stage 2 MHs. This poor correspondence was because of the difficulty in determining the size of the MP defect in stage 2 MHs. The retinal flap hampered determination of the exact area of the MP defect. Three parameters, that is, the diameter of the MP defect, minimum diameter of the MH, and maximum diameter of the MH, correlated with preoperative BCVA and final BCVA (Table 3).[26] Preoperative and final BCVA was worse in eyes with a larger diameter of these three parameters. Among them, the minimum diameter of the MH had the highest correlation coefficient; therefore, the significance of the size of the MP defect as a predictor of visual acuity in MH cases may be lower than that of the minimum MH diameter.

Vitreofoveal traction is generally considered to be the main cause of MH.[22,27] From close observation by biomicroscopy, Gass suggested that the change from a yellow spot to a yellow ring in the center of the fovea is an initial sign of MH development.[22]

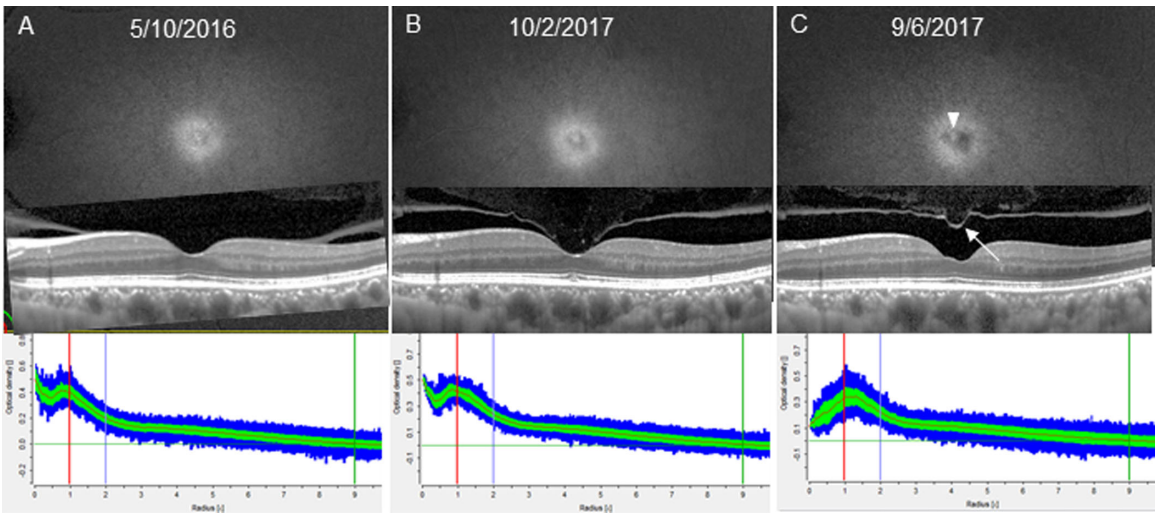

Figure 8. Fellow eye of the patient shown in Figure 4. MP distribution image (*top*), OCT images of the horizontal section (*middle*). The mean MPOD profile (*bottom*). (A) In October 2016, no posterior vitreous detachment is noted and MP shows a ring-like distribution. The pigment profile has two peaks. (B) In February 2017, posterior vitreous detachment starts to develop, but MP still shows a ring-like distribution. (C) In June 2017, complete posterior vitreous detachment is noted with a pseudo-operculum (*arrow*). MP shows central-dip distribution, and the pseudo-operculum contains pigment (*arrow head*). The foveal depression shows an irregular curvature.

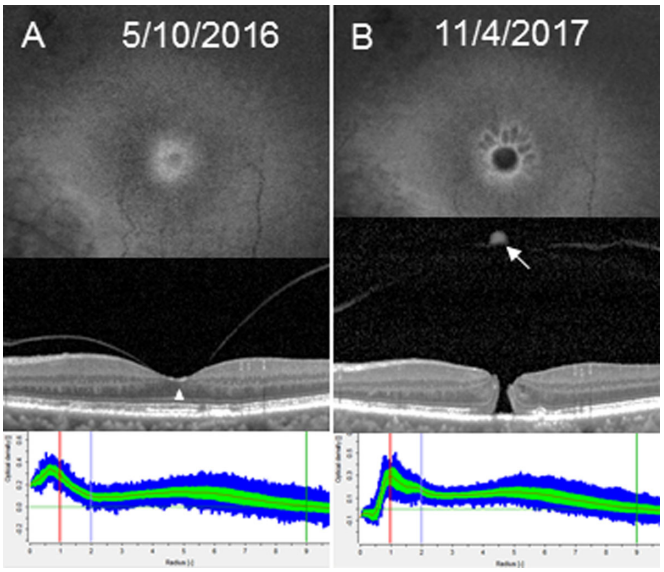

Figure 9. Left eye. MP distribution image (*top*), OCT images of the horizontal section (*middle*), and the mean MP density profile (*bottom*). (A) In October 2016, incomplete posterior vitreous detachment is noted, and MP shows a central-dip distribution. Irregular hyperreflectivity is observed at the foveal depression (*arrow head*). (B) In April 2017, MH developed. The *arrow* indicates the operculum.

He described that a yellow ring was formed by the centrifugal displacement of paracentral retinal receptors and xanthophyll, caused by tangential vitreofoveal traction, and it was accompanied by foveal detachment. A small dehiscence occurs in a yellow ring and progresses to MH. He claimed that 75% of cases of MH were associated with a prehole opacity that resembles pseudo-opercula and that prehole opacity was composed of vitreous cortical collagen, ILM, and Müller cell processes. Four years later, Gass emphasized the importance of the Müller cell cone that might contain MP and functioned to adhere the retinal receptor cells at the foveal center.[3] Considering the theory of the mechanisms of MH formation combined with Müller cell cone concepts, Gass suggested that vitreofoveal traction induces centrifugal migration of Müller cells that contain MP, and that a yellow ring is observed biomicroscopically. The disruption of the Müller cell cone leads to dehiscence of the central fovea and proceeds to MH development. According to this hypothesis, we thought that the origin of a central dip of MP was a centrifugal displacement of Müller cells by vitreofoveal traction, or a defect of the superficial part with pseudo-opercula by PVD (Fig. 6). When the PVD is incomplete and tractional force still exists, as shown in Figure 9A, the eyes with a damage to the Müller cell cone, that is, the eyes with a central dip of MP, develop MHs. In eyes with complete PVD, as shown in Figure 8C, the incidence of MH development is probably low.[28] In our previous study,[11] the rate of central-dip distribution was 12.5% in the healthy population; in contrast, the rate was 40% (10 of 25 eyes) in the fellow eyes of the present MH patients. This result indirectly suggests that subjects who developed MHs tended to have had a damage to the Müller

cell cone. The evaluation of MP distribution may be useful for identifying early changes in the foveal structure that induce MH formation.

MHs close by proliferation of Müller cells and reapposition of retinal tissue at the edge of the MH.[29,18,30,31] The MP profile in closed MHs showed a dense pigment spot at or near the center of the MP plane. The origin of the dense pigment spot was unclear, but the pigment spot resembled the central peak of the ring-like distribution type. We considered that the central peak of the ring-like type was formed by Müller cells at the foveal center.[11] Therefore, a dense pigment spot was probably produced by the recovered Müller cells at the fovea. Because the hypopigmented lesion in the MP plane corresponded with the defect of the OPL (Fig. 4), the MP plane itself was considered to depend largely on MP in the OPL. Because there was no change in the MPOV before and after surgery (Fig. 7), MP in the damaged Müller cell cone was quantitively less than that in the plexiform layers. The shape of the MP plane showed long-term changes. This result suggested that the tissue repair by Müller cell proliferation and reconstruction of sensory systems continues for a long time. The thickness of the retina differs between the nasal side and temporal side of the fovea after surgical closure of MH.[32] The difference in MP volume between the nasal and temporal sides was considered to be because of the differences in retinal thickness. The total MP volume was higher in the nasal side, which was thicker, than in the temporal side.

Pathology in the retina such as cystoid space in the outer layer and disruption of ELM and ellipsoid zone was repaired in the long term (Table 1) and the BCVA improved gradually (Fig. 2). In contrast, MP reaccumulated at week 2 and retained the same level until year 2 (Fig. 6). These results suggested no correlation between BCVA or pathologic changes in the outer retina and MP. Actually, there was no significant difference in MPOV between eyes with and without pathologic changes in the outer retina, and no correlation was observed between BCVA and MPOV. These findings are similar to a previous report.[6]

This study had a few limitations. Because the present SPECTRALIS software used to produce MP images does not have a function to measure the size of an area, we used image J to measure the size of the MP defect in MHs. However, small errors occurred in adjusting the sizes of MP images and OCT images, and the line on which the diameter was measured was not identical between MP and OCT images. Therefore, the concordance rates between MP defect and the minimum and maximum diameter of MH should be confirmed in further study by analyzing MP and OCT using the same image software. The correct determination of the edge of the OPL in MHs was difficult because of the resolution limit of OCT B-scan images. There were some errors in the value of diameters of the OPL defect. We presumed that a central dip in the MP image represented the damage to Müller cell cone caused by vitreofoveal traction based on OCT findings and hypothesis by Gass,[3,22] but this presumption needs histologic investigation. The damage to Müller cell cone may be induced by not only vitreofoveal traction, but also another mechanism such as degenerative change in Müller cells as reported in lamellar MH.[33] A MH developed in the eye with a central dip of MP, but this finding was confirmed in only one eye. Furthermore, it has been known that the concentrations of zeaxanthin and meso-zeaxanthin are high compared with lutein at the foveal center,[34] and it is suggested that the central dip correlates with a low serum zeaxanthin concentration and may be a risk factor for the development of age-related macular degeneration, because less MP owing to central dip induces intense photooxidative damage on the cone cells.[35] Therefore, the significance of the central-dip distribution as a predictor of MH formation has to be investigated in more cases in future studies.

The characteristics of MP in a MH were attributed to the anatomic changes in the Müller cell cone and plexiform layers. MP changes supported some speculations based on previous biomicroscopic and histopathologic studies. Observation of MP distribution was considered useful not only for understanding the mechanisms of formation and closure of MH but also for predicting MH formation.

Acknowledgments

Disclosure: **A. Obana**, None; **R. Nakazawa**, None; **S. Noma**, None; **H. Sasano**, None; **Y. Gohto**, None

References

1. Snodderly DM, Auran JD, Delori FC. The macular pigment. II. Spatial distribution in primate retinas. *Invest Ophthalmol Vis Sci*. 1984;25:674–685.
2. Yamada E. Some structural features of the fovea centralis in the human retina. *Arch Ophthalmol*. 1969;82:151–159.
3. Gass JD. Muller cell cone, an overlooked part of the anatomy of the fovea centralis: hypotheses concerning its role in the pathogenesis of macular hole and foveomacualr retinoschisis. *Arch Ophthalmol*. 1999;117:821–823.

4. Obana A, Sasano H, Okazaki S, Otsuki Y, Seto T, Gohto Y. Evidence of carotenoid in surgically removed lamellar hole-associated epiretinal proliferation. *Invest Ophthalmol Vis Sci*. 2017;58:5157–5163.
5. Neelam K, O'Gorman N, Nolan J, O'Donovan O, Au Eong KG, Beatty S. Macular pigment levels following successful macular hole surgery. *Br J Ophthalmol*. 2005;89:1105–1108.
6. Bottoni F, Zanzottera E, Carini E, Cereda M, Cigada M, Staurenghi G. Re-accumulation of macular pigment after successful macular hole surgery. *Br J Ophthalmol*. 2016;100:693–698.
7. Berendschot TT, van Norren D. Macular pigment shows ringlike structures. *Invest Ophthalmol Vis Sci*. 2006;47:709–714.
8. Dietzel M, Zeimer M, Heimes B, Pauleikhoff D, Hense HW. The ringlike structure of macular pigment in age-related maculopathy: results from the Muenster Aging and Retina Study (MARS). *Invest Ophthalmol Vis Sci*. 2011;52:8016–8024.
9. Sharifzadeh M, Bernstein PS, Gellermann W. Nonmydriatic fluorescence-based quantitative imaging of human macular pigment distributions. *J Opt Soc Am A Opt Image Sci Vis*. 2006;23:2373–2387.
10. Sharifzadeh M, Zhao DY, Bernstein PS, Gellermann W. Resonance Raman imaging of macular pigment distributions in the human retina. *J Opt Soc Am A Opt Image Sci Vis*. 2008;25:947–957.
11. Obana A, Gohto Y, Sasano H, et al. Spatial distribution of macular pigment estimated by autofluorescence imaging in elderly Japanese individuals. *Jpn J Ophthalmol*. 2020;64:160–170.
12. Meyer zu Westrup V, Dietzel M, Pauleikhoff D, Hense HW. The association of retinal structure and macular pigment distribution. *Invest Ophthalmol Vis Sci*. 2014;55:1169–1175.
13. Michalewska Z, Michalewski J, Adelman RA, Nawrocki J. Inverted internal limiting membrane flap technique for large macular holes. *Ophthalmology*. 2010;117:2018–2025.
14. Park SW, Pak KY, Park KH, Kim KH, Byon IS, Lee JE. Perfluoro-n-octane assisted free internal limiting membrane flap technique for recurrent macular hole. *Retina*. 2015;35:2652–2656.
15. Hangai M, Ojima Y, Gotoh N, et al. Three-dimensional imaging of macular holes with high-speed optical coherence tomography. *Ophthalmology*. 2007;114:763–773.
16. Michalewska Z, Michalewski J, Cisiecki S, Adelman R, Nawrocki J. Correlation between foveal structure and visual outcome following macular hole surgery: a spectral optical coherence tomography study. *Graefes Arch Clin Exp Ophthalmol*. 2008;246:823–830.
17. Kang SW, Lim JW, Chung SE, Yi CH. Outer foveolar defect after surgery for idiopathic macular hole. *Am J Ophthalmol*. 2010;150:551–557.
18. Michalewska Z, Michalewski J, Nawrocki J. Continuous changes in macular morphology after macular hole closure visualized with spectral optical coherence tomography. *Graefes Arch Clin Exp Ophthalmol*. 2010;248:1249–1255.
19. Akuffo KO, Nolan JM, Stack J, et al. The impact of cataract, and its surgical removal, on measures of macular pigment using the Heidelberg Spectralis HRA+OCT MultiColor device. *Invest Ophthalmol Vis Sci*. 2016;57:2552–2563.
20. Obana A, Gellermann W, Gohto Y, et al. Reliability of a two-wavelength autofluorescence technique by Heidelberg Spectralis to measure macular pigment optical density in Asian subjects. *Exp Eye Res*. 2018;168:100–106.
21. Green-Gomez M, Bernstein PS, Curcio CA, Moran R, Roche W, Nolan JM. Standardizing the assessment of macular pigment using a dual-wavelength autofluorescence technique. *Transl Vis Sci Technol*. 2019;8:41.
22. Gass JDM. Reappraisal of biomicroscopic classification of stages of development of a macular hole. *Am J Ophthalmol*. 1995;119:752–759.
23. Pang CE, Spaide RF, Freund KB. Epiretinal proliferation seen in association with lamellar macular holes: a distinct clinical entity. *Retina*. 2014;34:1513–1523.
24. Ezra E, Munro PM, Charteris DG, Aylward WG, Luthert PJ, Gregor ZJ. Macular hole opercula. Ultrastructural features and clinicopathological correlation. *Arch Ophthalmol*. 1997;115:1381–1387.
25. Li B, George EW, Rognon GT, et al. Imaging lutein and zeaxanthin in the human retina with confocal resonance Raman microscopy. *Proc Natl Acad Sci U S A*. 2020;117:12352–12358.
26. Ullrich S, Haritoglou C, Gass C, Schaumberger M, Ulbig MW, Kampik A. Macular hole size as a prognostic factor in macular hole surgery. *Br J Ophthalmol*. 2002;86:390–393.
27. Ezra E. Idiopathic full thickness macular hole: natural history and pathogenesis. *Br J Ophthalmol*. 2001;85.102–108.
28. Akiba J, Kakehashi A, Arzabe CW, Trempe CL. Fellow eyes in idiopathic macular hole cases. *Ophthalmic Surg*. 1992;23:594–597.
29. Madreperla SA, Geiger GL, Funata M, de la Cruz Z, Green WR. Clinicopathologic correlation of a macular hole treated by cortical

vitreous peeling and gas tamponade. *Ophthalmology*. 1994;101:682–686.
30. Bottoni F, De Angelis S, Luccarelli S, Cigada M, Staurenghi G. The dynamic healing process of idiopathic macular holes after surgical repair: a spectral-domain optical coherence tomography study. *Invest Ophthalmol Vis Sci*. 2011;52:4439–4446.
31. Bikbova G, Oshitari T, Baba T, Yamamoto S, Mori K. Pathogenesis and management of macular hole: review of current advances. *J Ophthalmol*. 2019;2019:3467381.
32. Ohta K, Sato A, Fukui E. Retinal thickness in eyes with idiopathic macular hole after vitrectomy with internal limiting membrane peeling. *Graefes Arch Clin Exp Ophthalmol*. 2013;251:1273–1279.
33. Govetto A, Dacquay Y, Farajzadeh M, et al. Lamellar macular hole: two distinct clinical entities? *Am J Ophthalmol*. 2016;164:99–109.
34. Bone RA, Landrum JT, Friedes LM, et al. Distribution of lutein and zeaxanthin stereoisomers in the human retina. *Exp. Eye Res*. 1997;64:211–218.
35. Trieschmann M, Spital G, Lommatzsch A, et al. Macular pigment: quantitative analysis on autofluorescence images. *Graefes Arch Clin Exp Ophthalmol*. 2003;241:1006–1012.